JOURNAL OF THE MECHANICAL BEHAVIOR OF BIOMEDICAL MATERIALS 60 (2016) 603–616

Available online at www.sciencedirect.com

ScienceDirect

www.elsevier.com/locate/jmbbm

Research paper

Characterisation of human diaphragm at high strain rate loading

Piyush Gaur[a], *Anoop Chawla*[a,*], *Khyati Verma*[a], *Sudipto Mukherjee*[a], *Sanjeev Lalvani*[b], *Rajesh Malhotra*[b], *Christian Mayer*[c]

[a]*Department of Mechanical Engineering, Indian Institute of Technology, New Delhi 110016, India*
[b]*All India Institute of Medical Sciences, New Delhi, India*
[c]*Daimler AG, 70546 Stuttgart, Germany*

ARTICLE INFO

Article history:
Received 8 September 2015
Received in revised form
12 February 2016
Accepted 25 February 2016
Available online 17 March 2016

Keywords:
Human soft tissues
Diaphragm
Impact
Strain rate dependence
Failure
Tensile characterisation

ABSTRACT

Motor vehicle crashes (MVC's) commonly results in life threating thoracic and abdominal injuries. Finite element models are becoming an important tool in analyzing automotive related injuries to soft tissues. Establishment of accurate material models including tissue tolerance limits is critical for accurate injury evaluation. The diaphragm is the most important skeletal muscle for respiration having a bi-domed structure, separating the thoracic cavity from abdominal cavity. Traumatic rupture of the diaphragm is a potentially serious injury which presents in different forms depending upon the mechanisms of the causative trauma. A major step to gain insight into the mechanism of traumatic rupture of diaphragm is to understand the high rate failure properties of diaphragm tissue. Thus, the main objective of this study was to estimate the mechanical and failure properties of human diaphragm at strain rates associated with blunt thoracic and abdominal trauma. A total of 23 uniaxial tensile tests were performed at various strain rates ranging from 0.001–200 s^{-1} in order to characterize the mechanical and failure properties on human diaphragm tissue. Each specimen was tested to failure at one of the four strain rates (0.001 s^{-1}, 65 s^{-1}, and 130 s^{-1}, 190 s^{-1}) to investigate the effects of strain rate dependency. High speed video and markers placed on the grippers were used to measure the gripper to gripper displacement. Engineering stresses reported in the study is calculated from the ratio of force measured and initial cross sectional area whereas engineering strain is calculated from the ratio of the elongation to the undeformed length (gauge length) of the specimen.The results of this study showed that the diaphragm tissues is rate dependent with higher strain rate tests giving higher failure stress and higher failure strains. The failure stress for all tests ranged from 1.17 MPa to 4.1 MPa and failure strain ranged from 12.15% to 24.62%.

*Corresponding author. Tel.: +91 11 26591058.
E-mail addresses: gaurhcst@gmail.com (P. Gaur), achawla@mech.iitd.ernet.in (A. Chawla), khyativermajss@gmail.com (K. Verma), sudipto@mech.iitd.ernet.in (S. Mukherjee), drsanjeevlalwani@gmail.com (S. Lalvani), rmalhotra62@hotmail.com (R. Malhotra), christian.c.mayer@daimler.com (C. Mayer).

http://dx.doi.org/10.1016/j.jmbbm.2016.02.031
1751-6161/

1. Introduction

Automotive safety research has been of interest to automotive designers over the last sixty years and remains an active area of study (Murray and Lopez, 1996). Automotive trauma continues to be major health challenge and often overlooked by the government. Motor vehicle crashes (MVC's) cause about half a million deaths annually throughout the world, which are about 30–50% of all injury related fatalities. Motor vehicle crashes commonly result in life threating blunt thoracic and abdominal injuries (Markogiannakis et al., 2006). In order to improve occupant protection, it is important to understand thoracic and abdominal injuries(Cavanaugh and Walilko, 1996; Chung et al., 1999). Thoracic trauma is a frequent occurrence in automotive collisions, second only to head injuries in terms of overall fatalities and serious injuries experienced (Nahum and Melvin, 2002). Thoracic and abdominal impact leading to damage of the soft tissues like the heart, the lungs, the aorta, the liver and the lungs can lead to sudden death. Abdominal injuries account for only 3–5% of all injuries observed in MVCs, they comprise 8% of AIS 3+injuries, 16.5% of AIS 4+injuries and 21% of AIS 5+injuries (Augenstein et al., 1999; Elhagediab and Rouhana, 1998; Thomas and Frampton, 1999; Yoganandan et al., 2000).

Finite element models of the whole human body are used to understand loading mechanisms of vehicle occupants during a vehicle crash event and to reduce the risk of injuries by evaluating alternate safety systems. Realistic geometry and accurate material properties are required to predict the human body response for different boundary and loading conditions (Carew et al. 1968; Patel et al.1969). With increasing computational power, it has become computationally feasible to use detailed geometries and material models incorporating rate dependent properties in conjunction with explicit Finite Element codes. In recent years, some human body model development efforts include the HUMOS1 and HUMOS 2 European projects (Behr et al., 2003; Robin, 2001), total human body model for safety (THUMS) by Toyota Central Research Lab, Wayne State human body model (WHMBS) by Wayne State University and a GHBMC model developed by The Global Human Body Modelling Consortium. The biofidelity of these models relies on an anatomically accurate and detailed representation of human body segmental geometry and material characterisation of tissue. One of the significant limitations in predicting the human body behaviour in crash events using finite element human body models is the limited data on the dynamic response of soft tissues (Chawla et al., 2007). The lack of data on dynamic behaviour of human soft tissues is firstly because of the difficulty involved in obtaining human tissues for testing and secondly because there are no standard testing techniques for dynamic testing of soft tissues.

Soft tissues in the human body include skin, skeletal muscles, tendons, ligaments, blood vessels, diaphragm, fat, and cartilage. Internal organs like kidney, lungs, liver, brain tissue, etc are labelled as very soft tissues. Effective modelling of these soft tissues has been limited by the complexity of their biomechanical properties as they exhibit non-linear, inelastic, hetrogenous, anisotropic characteristics (Holzapfel, 2000; Miller, 2000). The nonlinearity and degree of anisotropy depends very much on the soft tissue considered and its topographic location in human body. The non-linear behaviour of soft tissues is strongly influenced by the concentration and structural arrangement of collagen and elastin fibres, ground substance (GS), and cells (Holzapfel, 2004). Soft tissues behaves anisotropically because of the fibres which tend to have a preferred direction. The physiological function of each soft tissue necessitates certain degree of structural anisotropy, which is generally realized by variable arrangements of the functional components (Decraemer et al., 1980; Fung, 1975).The tensile response of soft tissues is non-linear and tensile strength depends upon the strain rate. Soft tissue may undergo large deformations and also show viscoelastic behaviour (relaxation and/or creep), which has been associated with the shear interactions of collagen fibres with the matrix of GS (Minns et al., 1973). The diaphragm is one of the most important skeletal muscle for respiration having a bi-domed shape structure in which dense collagen fibres are arranged diagonally from lateral to medial direction. Mechanical response of diaphragm muscle in tension can be compared with the tensile stress–strain behaviour of skeletal muscle shown in Fig. 1. At rest, the fibres appear orientated in a random fashion; however, once a load is applied, the fibres stretch parallel to the load direction. Initially elastin fibres are thought to stretch in a linear fashion and, as the load further increases, the collagen fibres reorient in order to carry a greater proportion of load (Fig. 1). This occurs in toe region of the stress–strain curve. As the load increases, a transition from low to high stiffness occurs and is known as the strain stiffening effect where the fibres become over stretched and begin to rupture until failure occurs (Edsberg et al.,1999; Gallagher et al., 2012).

Knowledge of the mechanical properties of human tissues is important for developing computational human body models to be used for predicting injuries. Even though, a of a lot of work has been done on characterizing soft tissues in the last decades, a majority of the experiments conducted on human tissues so far have been limited to quasistatic loading conditions (Carter et al., 2001; Egorov et al., 2002; Kenedi, 1971). Additionally, most of the existing dynamic data in the

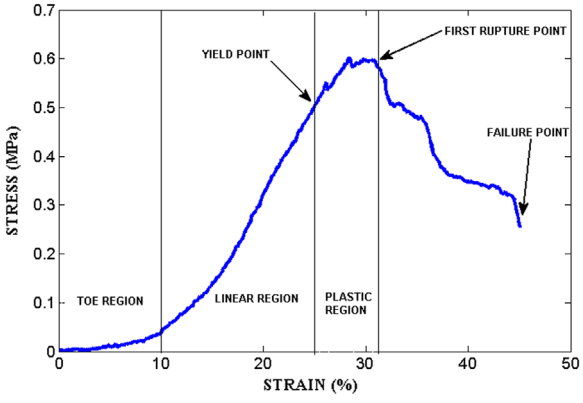

Fig. 1 – Typical stress–strain curve for tensile testing of skeletal soft tissue (Diaphragm). Collagen fibrils straightening and failure, related to different regions of the stress-strain curves, are also schematically shown.

literature has been obtained on porcine tissues (Snedeker et al., 2005a, 2005b) and some on bovine tissues (Chawla et al., 2005; Mavrilas et al., 2005; Warhatkar et al., 2009). Dynamic test data available in literature is typically limited to strain rates of the order of 10–100 s^{-1} (Mohan and Melvin, 1982, 1983; Rashid et al., 2012; Takaza et al., 2013), significantly lower then the strain rates that are estimated by models of impact on the body (Miller and Chinzei, 1997; Roberts et al., 2007). Few experimental studies on soft tissue properties have been conducted at high strain rates of the order of 1000–3800/s (Chawla et al., 2006; Ganpule et al., 2013; McElhaney, 1966; Saraf et al., 2007; Song et al., 2007; Taylor et al., 2014; Van Sligtenhorst et al., 2006) and also addressed injuries due to blast loading (Bartlett, 2003; Brown, 2014; Cooper et al.,1991; Covey, 2002; Laksari et al., 2014; Sellier and Kneubuehl, 1994). Capturing failure of soft tissues in impact like situations is an important aspect in predicting injuries. Most experimental data on dynamic failure of soft tissues were acquired using cadaveric tissues; to name a few, (Bir et al., 2004; Brunon et al., 2010, 2011; Butler et al., 1986; Kemper et al., 2012, 2010; Mattucci et al., 2012; Mohan and Melvin, 1982, 1983; Ottenio et al., 2015; Snedeker et al., 2005a, 2005b; Umale et al., 2013) had performed experiments on human kidney, liver, spleen, ureter, stomach, aorta, tendon, skin and ligament tissues. The force-time, deflection-time, and force–deflection responses of the chest to blunt ballistic impact have also been recorded using human cadavers (Yang et al., 1996). The response of thoracic wall and the lung to pressure waves has been simulated using an FE model (Grimal et al., 2004), throwing light on the mechanisms of transmissions of impact energy from the thoracic wall surface to the lung. Few authors like (Angelillo et al., 1997, 2000; Boriek et al., 2000, 2005; Kim et al., 1976; Margulies et al., 1994; Strumpf et al., 1993) have also studied the mechanics of active and tetanized canine diaphragm. They mention that the muscles bundles (fibres) of the diaphragm form a curved sheet that extends from the chest wall to the central tendon and that the functional force that balances the transdiaphragmatic pressure (Pdi), is exerted in the direction orthogonal to the surface (Kim et al., 1976). While these studies describe the pressure and stress distribution in the canine diaphragm or the response of other soft tissues (either porcine or cadaveric), to the authors knowledge, their have been no studies on the mechanical properties of human diaphragm tissues and their behaviour under high strain rate loading conditions like impact.

There are multiple types of soft tissues trauma, and these can result in complicated effects on physiological processes. Traumatic rupture of the diaphragm is one such potentially serious injury and presents in different forms depending upon the mechanism of the causative trauma. Diaphragmatic injuries (DIs) can occur following both blunt and penetrating trauma (Bosanquet et al., 2009). The incidence of diaphragmatic injuries have been reported as ranging from 1 to 7% with significant blunt trauma (Mihos et al., 2003; Scharff and Naunheim, 2007) and 10–15% with penetrating wounds in abdomen region (Adegboye et al., 2002). Traumatic injuries to the diaphragm is a relatively uncommon scenario, but few autopsy studies have recorded the incidence range of these injuries between 5.2% and 17% (Favre et al., 2005; Reber et al., 1998). Traumatic injuries of the diaphragm represent only 0.8–1.6% of the total lesions observed in blunt thoracic trauma (Mansour, 1997). A diaphragm injury is invariably a marker of serious trauma. The diaphragm is rarely injured alone, with an associated injury rate approaching 100% (Bosanquet et al., 2009). DIs are commonly associated with intra abdominal injuries, thoracic injuries, rib fractures, pelvis and long bones and rarely aortic injuries (Kara et al., 2004; McElwee et al., 1984). In the event of the death, it is commonly caused by a concomitant injury, rather than the diaphragmatic injury alone. Several mechanisms have been postulated for diaphragm injuries in blunt trauma (Hanna et al., 2008). These include avulsion of diaphragmatic attachements, shearing effects from lateral impact to the chest wall, rib fracture fragments penetrating the diaphragm, and sudden build up of force through the abdominal viscera acting as a hydrodynamic fluid leading to disruption. Road traffic collisions or lateral intrusions into the vehicle are the most common frequent causes of diaphragm rupture (Ahmad et al., 2015; Murray et al., 1998; Ozpolat et al., 2009; Reber et al., 1998). Direct impacts depress the side of the ribcage, and can cause a tear in the diaphragm rib attachements, and even the transverse rupture of the diaphragm (Boulanger et al., 1993). Serious slowdown pinching to diaphragm results in increase inter-abdominal pressure by ten time or more and if the the patient holds his/her breadth and contracts the abdominal wall during impact can cause severe diaphragm injury (Favre et al., 2005).There is a lack of proper constitutive model to model rupture of soft tissues reported in literature and this applies to diaphragm injuries as well. In order to accurately predict the rupture injuries in diaphragm, it is necessary to investigate the tensile mechanical properties of human diaphragm subjected at various strain rates. However, to the author's knowledge, there is no dynamic uniaxial or biaxial test data for diaphragm available in literature. Thus, the main objective of this study is to quantify the uniaxial tensile material properties of human diaphragm at various strain rates, i.e. up to 200/s.

2. Material and methods

2.1. *Sample preparation*

Uniaxial tensile tests were performed on 6 human diaphragm obtained from un-embalmed post mortem human subjects received from the All India Institute of Medical Sciences (AIIMS) and Jai Prakash Narayan Apex Trauma Centre, New Delhi after clearance from a duly approved ethics committee. Each specimen was obtained within 36–48 h of death. Subject gender, weight, age and height were documented (Table 1). Diaphragm samples were obtained from the right side of the body, particularly from the region near the upper right portion of the liver and were then stored at −20 °C prior to test. Before preparation and testing the specimens were thawed at room temperature in buffered saline solution for two hours.

The common specimen shapes that have been used for tensile testing of soft tissues are rectangular (strip) (Chawla et al., 2005; Christensen et al., 2015; Gao and Desai, 2010;

Table 1 – Subject information.

Human no	Gender	Age (years)	Weight (kg)	Height (cm)
1	Male	38	59	162
2	Male	55	60	155
3	Male	65	63	165
4	Male	45	NA	150
5	Male	60	50	158
6	Male	58	50	154

*NA – Not available.

Warhatkar et al., 2009) and dogbone shapes (Assari et al., 2014.; Duprey, 2008; Gallagher et al., 2012; Manoogian et al., 2008; Mattucci et al., 2012). Rectangular samples were used based on preliminary data from a separate set of goat diaphragm tissue using identical tensile test settings which showed consistent breakage at the midpoint in gauge length of the tissue (data not shown). Using dogbone shape specimen may induce disruptive effects on the continuity of fibres along the length at sites where change in cross-sectional area occurs. Employing a uniform rectangular strip ensures that the irregularities of the stress/strain fields are only limited to gripping effects. Therefore, to ensure consistency and ease in tissue preparation, rectangular samples have therefore been used in this study instead of dog-bone shaped samples.

Rectangular samples were obtained from diaphragm sheets using surgical scalpel (as shown in Fig. 2(a)–(d)). The width and length of the specimen was measured at four consecutive points. The thickness of the diaphragm membrane was measured at four random points using a caliper. The average thickness of diaphragm specimen recorded is 2.25 ± 0.5 mm. Specimen's details have been documented in Table 2. To ensure a shear free deformation and rupture of tissue within the gauge length of the specimen, an aspect ratio (AR corresponds to the gauge length divided by the width of the specimen) of 2 is suggested in literature (Duprey, 2008) for tensile testing of soft tissues. However, most experimental studies on tensile testing of soft tissues, to name a few (Assari et al., 2014; Christensen et al., 2015; Duprey, 2008; Egorov et al., 2002; Kemper et al., 2012, 2010; Manoogian et al., 2008; Ottenio et al., 2015; Rashid et al., 2014; Snedeker et al., 2005a, 2005b) have used aspect ratio between 1.3–2.5 for different body organs. Hence, an average aspect ratio of 1.9 is used in our tests to ensure uniform stress-strain field within the gauge length of the specimen.. After preparation, the samples were immersed in a saline solution at room temperature (24 °C). Time between sample preparation and tensile testing never exceeded 1 h. The tensile testing setups and sample preparation methodology was standardized by conducting quasi-static and dynamic tensile tests on goat diaphragm samples.

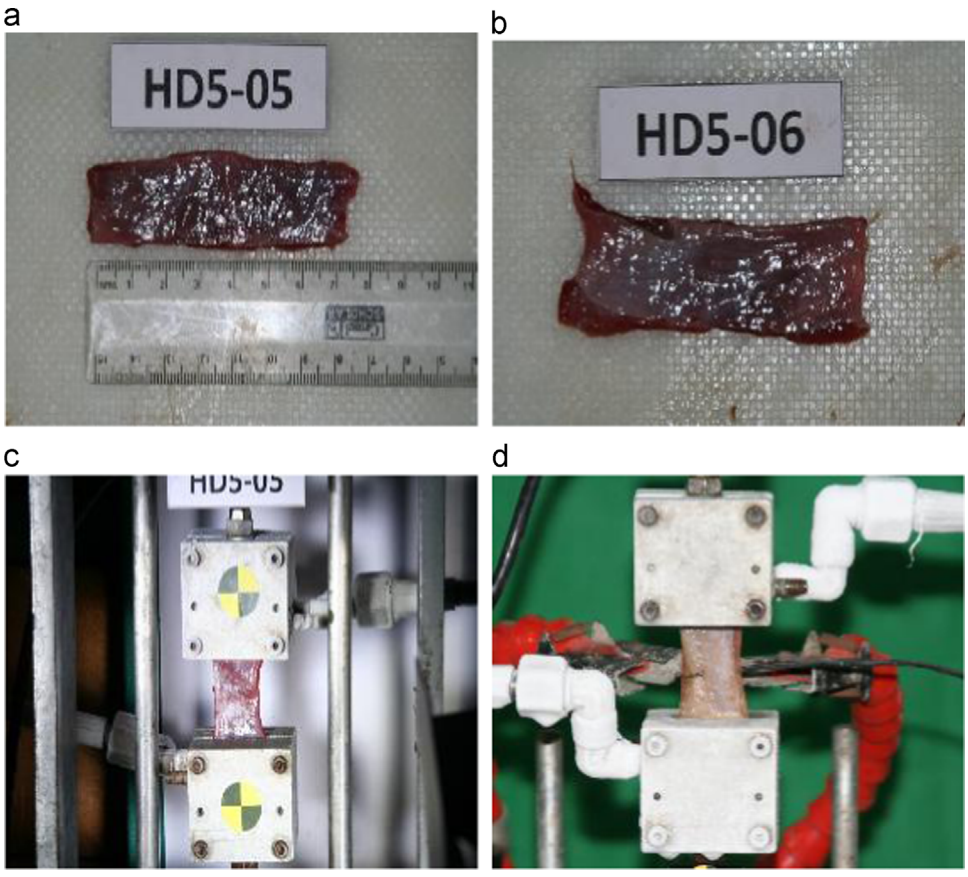

Fig. 2 – (a) Measurement of specimen length, (b) final sample for testing, (c) specimen mounted on tensile testing setup and (d) diaphragm specimen within cryogenic grippers (enlarged view).

Table 2 – Test matrix for human diaphragm used in quasi-static and dynamic tensile tests.

S. no	Test Id	Strain rate (/s)	Av. thickness (mm)	Av. width (mm)	Gauge length (mm)	C.S. area (mm^2)
1	HD1-01	0.001	2.55	20	38	51
2	HD1-02	0.001	2.69	22	30	59.74
3	HD1-03	0.001	2.58	24	35	63.08
4	HD1-04	0.001	2.61	23	30	61.22
5	HD2-01	68	2.52	22	44	57.27
6	HD2-02 (F)	65	3.5	21	46	76
7	HD2-03	69	2.36	20	37	47.2
8	HD2-04	130	2.23	20	40	44.6
9	HD2-05	67.56	2.65	20	37	53.1
10	HD2-06	136	3.2	20	33	64.1
11	HD2-07	125	2.85	18	45	51.12
12	HD2-08 (F)	190	2.3	20	30	45.4
13	HD2-09	180	2.21	18	31	39.69
14	HD3-01	190	1.53	24	27	30.85
15	HD3-02	190	1.88	21	28	38.96
16	HD3-03 (F)	190	1.7	22	30	37.82
17	HD5-01 (PR)	0.001	1.63	19	35	31.18
18	HD5-02 (PR)	0.001	1.8	16	27	29.05
19	HD5-03	0.001	1.3	17	29	22.22
20	HD5-04	130	1.9	20	34	39.21
21	HD5-06	130	2.28	23	40	52.32
22	HD6-01	190	1.6	21	35	33.2
23	HD6-02	190	1.8	24	29	42.63
		(Mean ± SD)	**2.25 ± 0.54**	**19 ± 2.13**	34 ± 5.6	34.34 ± 12.95

* F = Failed test, PR – Premature ruptured failed specimens

2.2. *Tensile tests*

Uniaxial tensile tests were performed on human diaphragm samples on a custom designed quasi-static and dynamic tensile system Fig. 3(a) and (b).

2.2.1. *Quasi-static tensile test set-up*

The quasi-static tensile test setup consists of a stepper motor driven screw in line with a worm and worm wheel is used to axially load the specimen. The screw can be driven at a constant rate between 0.5 mm/min and 3.68 mm/min to achieve a near zero strain rate. A nut transforms the rotary motion into translation motion of the lower gripper. The motor input is governed by a microcontroller with a local console. The diaphragm specimens were held using cryogenic grippers with liquid nitrogen flowing through them. Frost formed between the gripper faces and continuing into the specimen during holds the specimen during loading without local crushing and tears of the outer fibres. A temperature control unit regulates the midpoint temperature of the specimen using an on-off controlled hot air-flow. A flexible pipe, with variable opening area was used to adjust the flow of hot air over the gauge length of the specimen during the test. A laser sensor (Model number OADM 2014470/S14C, Baumer Electric) having resolution ≤ 0.3 mm, mounted on the guide rod of static lower gripper is used to measure the

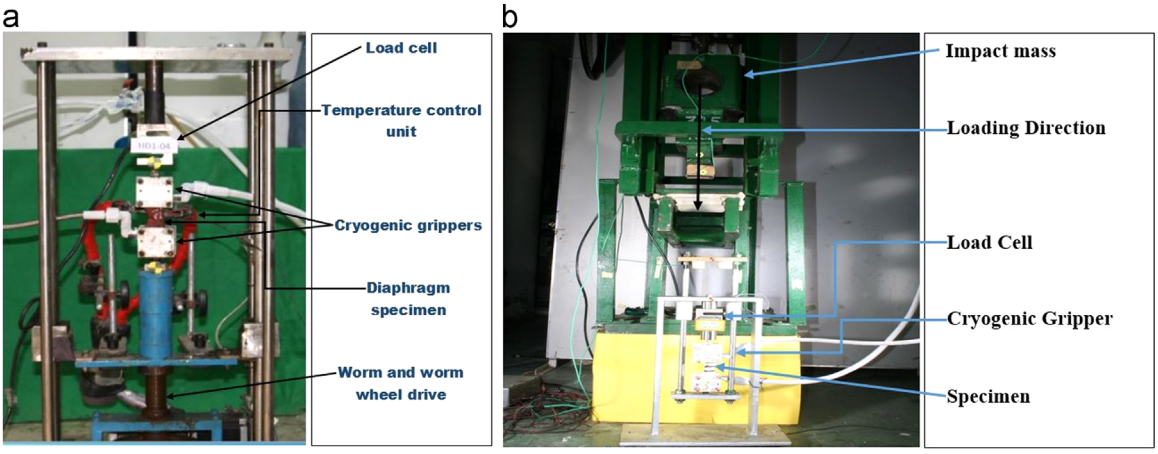

Fig. 3 – Tensile testing setups, (a) Quasi-static tensile test setup and (b) dynamic tensile testing setup (Warhatkar et al., 2009).

extension of the lower gripper during loading. A strain gauge load cell (Model 20210, ARTECH, S beam type) was used to measure the load on the specimen. Video recording of the tests at 100 fps was used for further analysis.

2.2.2. *Dynamic tensile test set-up*

A customised dynamic tensile drop test set up can load specimen at strain rates up to 200/s. The drop height generates a maximum velocity of 8 m/s. A drop mass of 30.5 kg was found to be sufficient to limit the energy during impact to 10%, or equivalently to 5% change in the velocity. The specimens were held in the same way as in the quasi-static tests using cryogenic grippers. A strain gauge based transducer from ADI ARTECH with a capacity of 100 kg, mounted on the top gripper is used to record the forces. Two high speed motion cameras were used to record the dynamic events. In this set up, one camera was used to zoom into the zone between the grippers while the other camera can be used to capture the jaw motion during the entire duration of impact. A buffered switch triggered by the impact was used to trigger the high speed camera and data acquisition system. It additionally synchronizes the recorded force and displacement data and hence to identify the start of the event recorded using data acquisition system from Dewesoft Corporation (2007). The sampling rates used to acquire load cell data and high speed video is 1 Sample/s and 60 frames/s respectively in quasi-static testing and 200 k Samples/s and 20,000 frames/s respectively in dynamic testing.

2.3. *Testing configuration and methodology*

In order to investigate strain rate dependence, each specimen was tested to failure at one of the four desired strain rates: 0.001 s^{-1}, 65 s^{-1}, 130 s^{-1}, or 190 s^{-1}. The procedure of mounting the specimens was same for quasi-static and dynamic tensile tests. To mount the specimens, the upper gripper assembly was first removed from the experimental setup and laid flat on the floor. The specimen was then aligned on the top grip so that the main axis of the specimen coincided with the axis of the lower gripper assembly and load train. The specimens after being placed in the top gripper were tightened with nuts and bolts to ensure no slipping of the specimens during loading. The top grip assembly was attached to the experimental set up after clamping and the specimen was then allowed to hang under gravity. By allowing the specimen to hang under their own weight during the clamping process, all the specimen had a minimal but consistent initial preload. The hanging tissue was then placed in the bottom gripper and clamped. Without this procedure, the mechanical responses of each specimen could not be directly compared due to the differences in the initial value of strain. The determination of a consistent initial state of strain due to the compliant nature of the soft tissues is an important issue associated with mechanical testing of soft tissues. In order to address this issue, some previous studies have defined the point of "*zero strain*" with some arbitrary force value (Tamura et al., 2002). However this differs in quasistatic and dynamic tests. Thus, in order to ensure that there is no slack in the specimen at the start of the test, the specimen was loaded to 2 kg in both quasi-static and dynamic tests. This condition was taken to be the zero stress–strain state of the specimen. This was done because preliminary tests done on goat diaphragm specimens showed inconsistent large toe region due under varying or zero initial specimen slack. Thus, the 2 kg preload used in the current study provided a consistent initial load on all specimens.

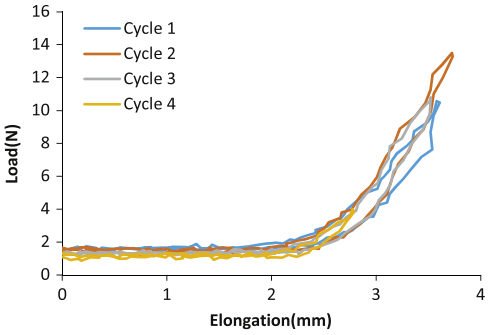

Fig. 4 – Preconditioning response of one of the diaphragm specimens.

In quasi-static tests, a thermocouple attached at the mid gripper location on the soft tissue sample was used in conjunction with a temperature control unit which was started before the start of loading to ensure constant temperature of the gauge portion of the specimen. The specimens were then preconditioned at the strain for 5% for 4–5 cycles prior to testing in order to prevent the macro or micro failure and to bring back the tissue in live state. Typical preconditioning response on one of the human diaphragm samples is shown in Fig. 4. The strain rate achieved in quasistatic tests was 0.001 s^{-1} corresponding to load rate of 3.68 mm/min with a pulse speed of 99. In dynamic tests, impact mass height and velocity was estimated as per as the targeted strain rate. For strain rate of 65 s^{-1}, the average velocity is about 2.5 m/s, 4.5 m/s for 130 s^{-1} and 6.1 m/s for 190 s^{-1} strain rates. Based upon the available specimen lengths, the test lengths varied between 29 mm and 46 mm in tests. Once the specimen were mounted, side view and front view photographs were taken. Markers placed on the grippers and high speed video was taken during the dynamic tests to measure the gripper to gripper displacement. Finally, photographs of ruptured tissues were also taken to record the failure pattern and location of failure with respect to the gripper edges.

2.4. *Data processing and analysis*

In order for a test to be deemed acceptable, the location of the failure must have occurred in the gauge length of the specimen. Therefore, specimens which slipped from any of the grippers were not included in the final results. Failure was defined either as a point at which a tear was seen in the high speed video or as the point where the load peaked preceding a significant decrease in load. Unfiltered force displacement data from both quasi-static and dynamic test data were obtained and processed. Gripper to gripper strain was quantified by first tracking the markers placed on the grippers throughout the duration of the test using image tracking software (Motion Studio, Integrated Design Tools Inc). The

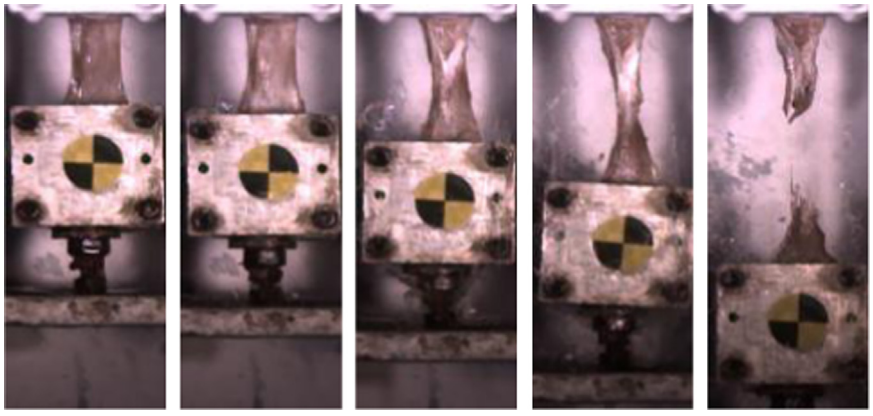

Fig. 5 – High speed video stills of a typical uniaxial dynamic tensile test.

load elongation curve was derived to obtain the stress-strain relationship. Assuming diaphragm to be an incompressible material and for small deformations, true stress and true strain values can be computed. However, both these assumptions are not valid in this case. The current work therefore uses engineering stress and engineering strain values. In the past researchers working on mechanical properties of soft tissues have used different stress–strain definition. (Gundiah et al., 2007; He and Roach, 1994; Raghavan et al.,1996; Thubrikar et al., 2001; Vorp et al., 2003), to name a few have used true stress versus engineering strain. (Chawla et al., 2006; Choudhury et al., 2009; Sokolis, 2007) on the other hand have used engineering stress versus engineering strain. Mohan and Melvin (1982) emphasised the importance of using true stress–strain definition for soft tissue testing, but recording true stress and true strain remains a concern.

The quasi-static and dynamic material properties of human diaphragm were then estimated by fitting a bilinear curve in the stress-strain curve obtained. The bilinear fit was obtained in Matlab^{TM} by minimising the root mean square of the error between the experimental and the approximated line using least square method.

3. Results and discussion

To the authors' knowledge, the current study is the first study to quantify the mechanical response of the human diaphragm tissue in tensile loading at strain rates up to 200/s. Uniaxial tensile tests were performed on 23 samples of human diaphragm tissue at strain rates ranging from 0.001 to 190 s^{-1}. Out of the 23 tests, a total of 18 tests were successful and the specimens had a rupture within the gauge length of the rectangular specimens (Fig. 5). The other tests have not been reported due to one or more recording device not triggering or premature failure of the specimen during testing. The stress versus strain curves from the specimens which failed in the gauge length are shown in Fig. 6–9.These curves show that the tensile response of human diaphragm was non-linear at all strain rates. The average failure stress, average failure strain and average strain rate are tabulated in Table 3. These parameters for all the tests are tabulated in the (Tables 4–7). The results show that the response of diaphragm in tensile loading is non-linear and varies with

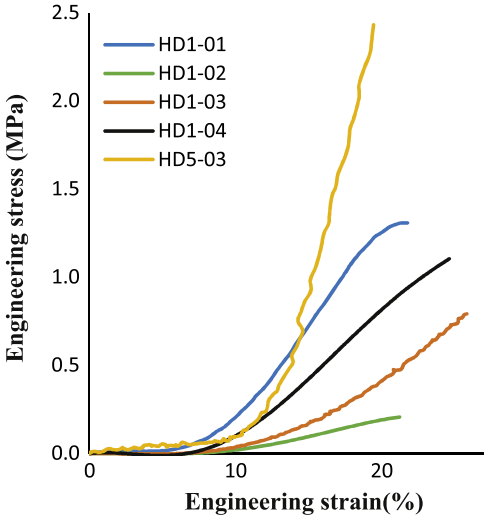

Fig. 6 – Stress vs. strain curves for quasi-static strain rate.

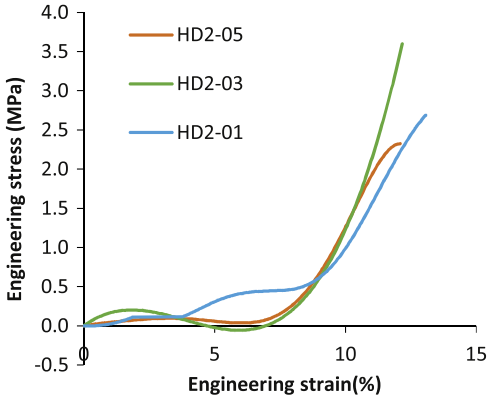

Fig. 7 – Stress vs. strain curve for 65/s strain rate.

respect to strain rate (Table 3). Specifically, the failure stress was found to increase with the increase in strain rate which is in accordence with the property of viscoelastic material. Conversely, the average failure strain was found to be decrease with increase in strain rate uptill 65/s strain rate and then increases upto 190/s strain rate. However,

significant difference was not observed at high strain rates, i.e. 130/s and 190/s for either failure stress or failure strain.

The elastic region of the stress strain response observed can be approximated by using bilinear curve as shown in Fig. 10. This is consistent with Fung (1975) that says that the modulus in the toe region, should also be taken into account as the toe region is usually the physiological range in which the soft tissue normally functions. Several authors have used bilinear model to approximate non-linear stress–strain curves (Lake et al., 2009; Mattucci et al., 2012; Mohammadi et al., 2009; Snedeker et al., 2005a; Warhatkar et al., 2009; Zhang and Kassab, 2007) to name a few. These studies have used the notion of the toe modulus to represent the physiological range and the elastic modulus thereafter for a range of body organs. Hence, a bilinear stress strain behaviour has been used in the current work to capture the non-linear behaviour of human diaphragm tissue. The bilinear fit was obtained in Matlab™ by minimising the root mean square of the error between the experimental and the approximated line using least square method. The bilinear fits obtained for stress-strain curves are is shown in Figs. 11–14 for the different strain rates. These curves are characterized by a low stiffness "toe" region, which is approximately up to 8.59–14% engineering strain. Thereafter, the modulus increases, an effect which can be attributed to progressive fibres recruitment. Once the fibres are recruited, the curve becomes linear. This linear behaviour continues until just before tissue rupture. The bilinear material curves observed in both quasi-static and dynamic tests were reduced to the characteristics material parameters: Toe modulus (E_1), Elastic modulus (E_2), Failure Stress (σ_f), Failure strain (ϵ_f) and Toe strain (ϵ_t). These parameters were observed for their dependence on strain rate.

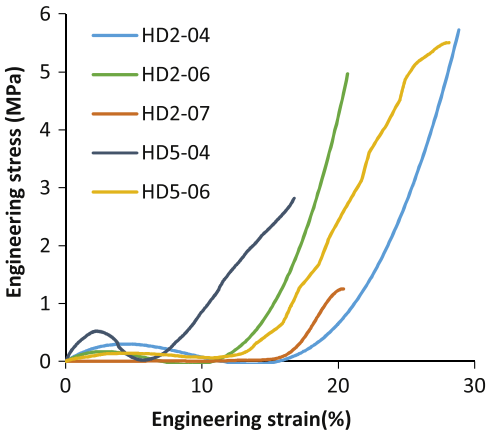

Fig. 8 – Stress vs. strain Curves for 130/s strain rate.

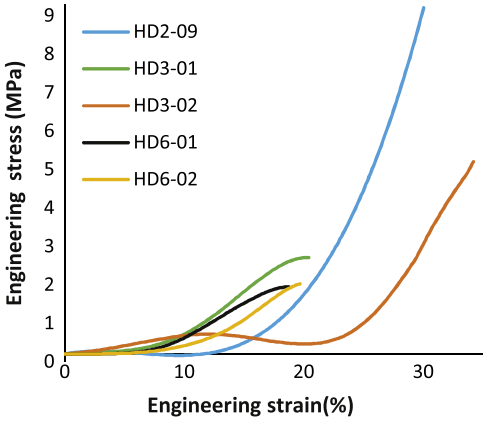

Fig. 9 – Stress vs. strain Curves for 190/s strain rate.

Table 3 – Averages and standard deviations by strain rate.

Strain rate	Average strain rate (/s)	Average failure stress (MPa)	Average failure strain (%)
Rate 1	0.001	1.17 (±0.73)	22.35(±2.35)
Rate 2	66 (±1.65)	2.53(±0.16)	12.19(±0.67)
Rate 3	130 (±3.90)	3.98(±1.84)	22.92(±5.27)
Rate 4	188 (±4.72)	4.1(±2.78)	24.62 (±6.30)

It is observed from Fig. 6, that the diaphragm specimens exhibit non-linear behaviour in quasi-static loading with a significant toe region. The elastic modulus under quasi-static conditions was noted to be 11.5±11.44 MPa. The failure stress and failure strain were observed to be 1.17±0.53 MPa and 22.5±2.5% respectively. The failure stress observed for diaphragm specimens (HD1-01, HD1-02, HD1-03 and HD1-04) was observed to be between 0.2 MPa and 1.4 MPa, however the failure stress recorded for specimen (HD5-03) was 2.53 MPa which was quite high as compared to other three specimens. The modulus for this specimen was also higher than that for others. However, no significant difference was observed in case of failure strain in these specimens. This variation in failure stress and modulus could be because of inherent variations in properties of tissues amongst donors. More extensive tests would need to be conducted to characterize these variations. Additionally, the response has a distinct toe region which in quasi-static tests is up to about 8–12.5% strain. The average toe strain at quasi-static strain rate is 10.4±1.98%. A similar trend in toe region is observed in

Table 4 – Mechanical properties for diaphragm at quasi-static strain rate.

S. no	Test Id	Strain rate (/s)	Toe modulus (MPa)	Elastic modulus (MPa)	Toe strain (%)	Failure strain (%)	Failure stress (MPa)
1	HD1-01	1.00E−03	0.82	9.4	8.13	21.77	1.35
2	HD1-02	1.00E−03	0.069	1.79	9.86	21.04	0.21
3	HD1-03	1.00E−03	0.38	5.71	12.83	25.84	0.8
4	HD1-04	1.00E−03	0.111	6.79	8.71	24.64	1.09
5	HD5-03	1.00E−03	1.27	33.88	12.74	19.45	2.43
	Mean±SD	1.00E−03	0.53±0.46	11.51±11.44	10.45±1.98	22.55±2.35	1.17±0.73

Table 5 – Dynamic mechanical properties of human diaphragm at 65/s strain rate.

S. no	Test Id	Strain rate (/s)	Toe modulus (MPa)	Elastic modulus (MPa)	Toe strain (%)	Failure strain (%)	Failure stress (MPa)
1	HD2-01	65	6.1	56.1	9.21	13.06	2.68
2	HD2-03	65	1.4	86.71	8.56	11.43	2.61
3	HD2-05	67.86	1.51	51	7.76	12.09	2.32
	Mean ± SD	66 ± 1.65	3.0 ± 2.19	64.6 ± 15.76	8.59 ± 0.59	12.19 ± 0.67	2.53 ± 0.16

Table 6 – Dynamic mechanical properties of human diaphragm at 130/s strain rate.

S. no	Test Id	Strain rate (/s)	Toe modulus (MPa)	Elastic modulus (MPa)	Toe strain (%)	Failure strain (%)	Failure stress (MPa)
1	HD2-04	130	1.51	69.03	21	28.83	5.60
2	HD2-06	136	1.62	79	14.71	20.69	4.85
3	HD2-07	125	0.1924	31.11	9.24	20.37	1.35
4	HD5-04	130	4.04	28.6	8.04	16.76	2.82
5	HD5-06	130	1.51	42.77	14.72	28.11	5.4
	Mean ± SD	130.2 ± 3.90	1.77 ± 1.40	50.10 ± 22.74	13.54 ± 5.18	22.95 ± 5.27	4.00 ± 1.84

Table 7 – Dynamic mechanical properties of human diaphragm at 190/s strain rate.

S. no	Test Id	Strain rate (/s)	Toe modulus (MPa)	Elastic modulus (MPa)	Toe strain (%)	Failure strain (%)	Failure stress (MPa)
1	HD2-09	180	2.13	84.62	20.14	30.04	9.10
2	HD3-01	190	1.96	18.32	7.48	20.41	2.52
3	HD3-02	192	2.43	49.31	25.36	34.2	5
4	HD6-01	190	0.6107	14.4	6.9	18.75	1.75
5	HD6-02	190	1.4	18.76	10.75	19.69	1.83
	Mean ± SD	188.4 ± 4.72	1.71 ± 0.70	37.10 ± 26.88	14.12 ± 7.35	24.62 ± 6.29	4.10 ± 2.78

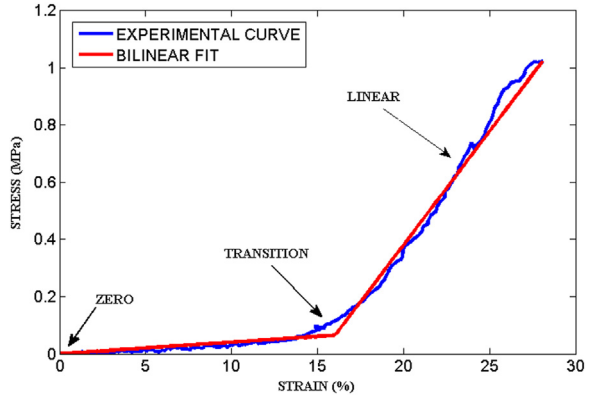

Fig. 10 – Example bilinear curve fit of diaphragm stress-strain tensile data; arrows indicate the zero, transition and linear strain values.

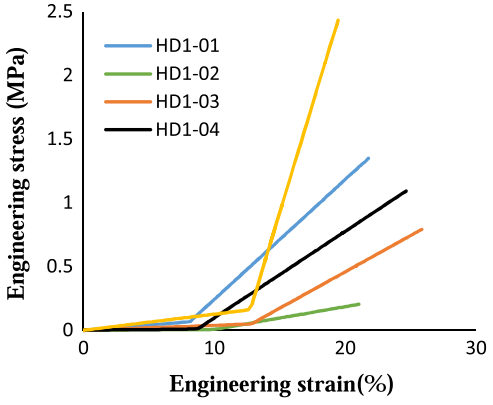

Fig. 11 – Bilinear curves for 0.001/s strain rate.

case of dynamic tests as well. The toe strain noted in dynamic strain rates was 8.59 ± 0.59% for 65/s, 13.54 ± 5.18% at 130/s and 14.12 ± 7.35% for 190/s strain rates. The toe strain was observed to decrease up to 8.59% for 65 strain rate which increased to 13.54% for 130 and 14.12% at 190 strain rate which again proves that there is an increase in toe strain with strain rates. The failure stress for diaphragm tissue at 65/s strain was observed to be 2.68 MPa, 2.6 MPa and 2.32 MPa. In one test each conducted at 65 and 130/s strain rates, a slight negative dip of engineering stresses is observed (HD2-03 at 65/s, HD2-04 at 130/s, which could be because of experimental variations or signal processing issues. The average failure stress is 3.98 MPa for 130/s strain rate and 4.10 MPa at 190/s strain rate. A low value of failure stress of 1.35 MPa, 1.75 MPa and 1.83 MPa was noted in some cases of 130/s and 190/s strain rate respectively. This variation in case of failure stress could be because of variations in properties of tissues

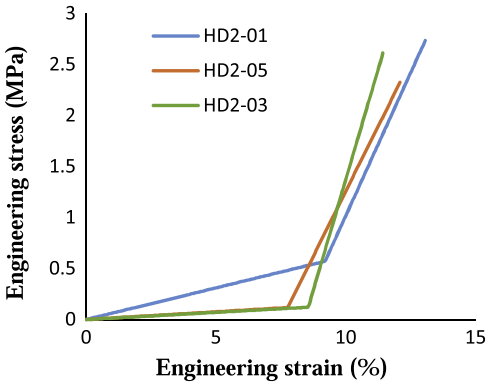

Fig. 12 – Bilinear curves for 65/s strain rate.

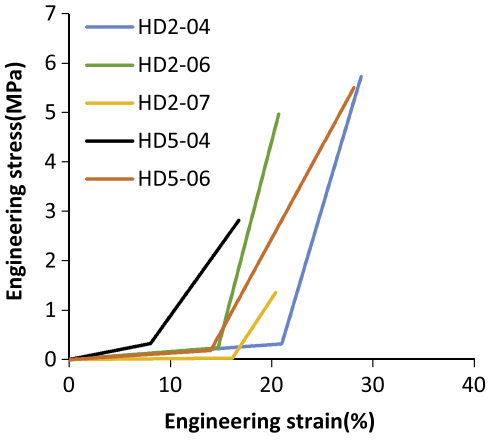

Fig. 13 – Bilinear fit for 130/s strain rate.

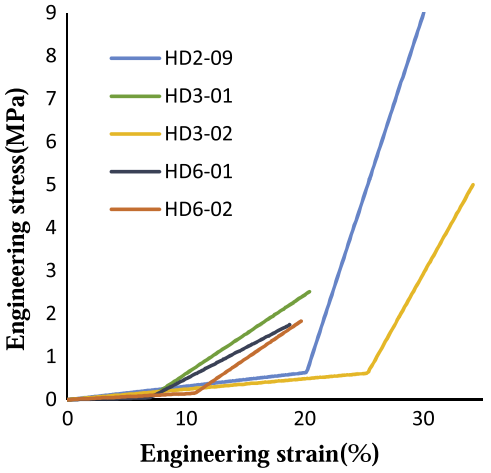

Fig. 14 – Bilinear fit for 190/s strain rate.

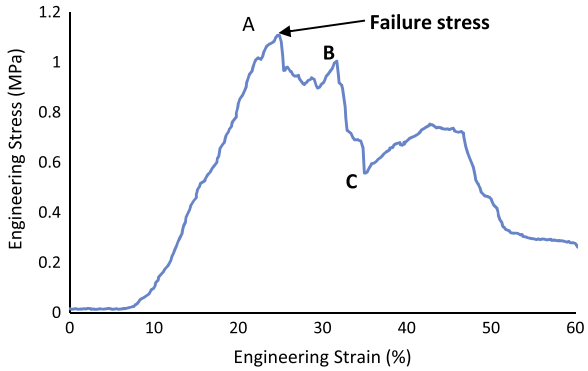

Fig. 15 – Stress strain plot of quasi-static test (HD1-04).

amongst donors. The failure stress observed to have increased with the increase in strain rate which is in accordance with the property of viscoelastic material. However, a substantial difference in failure strain is being noted. The average failure strain at 65/s strain rate was observed to be 12.2% at 65/s, 22.95% at 130/s strain rate and 24.62% for 190/s strain rate. In one of the tests conducted at 190/s strain rate, the failure strain was observed to be around 34%. Also, a slight differences in the failure stain values at 130/s and 190/s strain rate is also noted. The difference in such a variation could be due to internal fibres bearing load for a longer duration and then got ruptured immediately. As stated earlier, more extensive tests would need to be conducted to characterize these variations.

In both the quasi-static and dynamic tests the diaphragm specimen have exhibited a peak stress which is assumed to be the failure stress. At this failure point, the diaphragm undergoes a partial failure, not a complete rupture of the tissue. In some of the tests, the failure at failure stress point is not visible from surface observations. A typical complete stress–strain curve is shown in Fig. 15 (that corresponds to the test HD1-04) so as to explain the sequence of loading to failure of diaphragm tissue. In this curve, stress peaks at point “A”. At this point, a few fibres of diaphragm are seen to fail. From point B to C, further rupture takes place which is accompanied by a sudden sharp drop in load. Multiple dips in the stress strain curve indicate selective failure of diaphragm fibres in different stages. This is probable because of non-uniform stress and strain in the individual fibres across the width of the specimen. Fibres of the diaphragm fail in groups at different locations along the gauge length and width of the specimen. Because of this, the rupture of the diaphragm does not happen suddenly but happens progressively after point “A”. From these tests it is also noted that the failure occurred away from the cryogenic grippers. This proves a point that the holding devices did not induce the rupture of diaphragm.

The reduced material parameters as a result of bilinear fit explained above were analysed to identify the influence of strain rate on the mechanical behaviour of this tissue. The apparent toe modulus, elastic modulus, failure stress, toe strain, failure strain along with their average values for each strain rate are tabulated in (Tables 4–7). Tables 4–7 show that with increasing strain rate the failure stress stresses increases and failure strain increases significantly with increased strain rate. The trend observed in failure strain was not significant between all loading rates in the current study, in the current study, however, it does indicate that the strain rate dependency should be taken into account when developing material models or injury thresholds for soft tissues. The results of the tests show that the response of the human diaphragm in tensile loading is nonlinear. The variation of elastic modulus, failure stress and failures strain with respect to strain rate is shown in Fig. 16. It can be

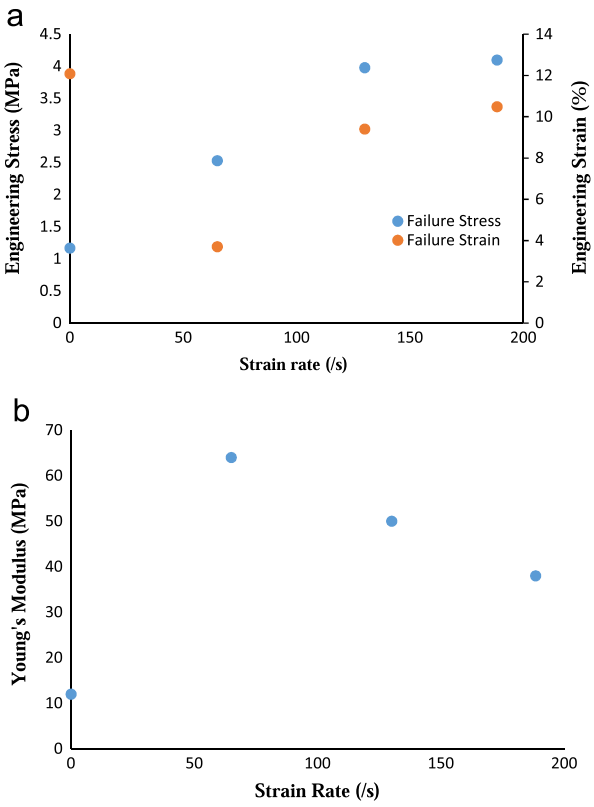

Fig. 16 – (a) Failure stress and failure strain variation and (b) Young's Modulus variation wrt strain rate.

observed from above Fig. 16(b) that the value of Young's Modulus varies between 11 MPa and 64.6 MPa with increasing trend upto 65/s strain rate and further decreases to 38 MPa at 190/s strain rate. This could be because of regional variation in mechanical properties of human diaphragm. This would, however, be investigated when more data is available in near future. In addition, the results show that diaphragm tissue exhibits viscoelasticity in tensile loading. Specifically, the failure stress was found to significantly increase with increased strain rate and the failure strain was found to vary marginally with increase in strain rate. The failure strain in case of quasi-static tests was recorded as 22% which decreases subsequently to 12.25% at 65/s and then increases to 24.6% at 190/s strain rate. The variation in failure strain can be quantified more reliably by performing more tests on human diaphragm.

From the above stress–strain curves of human diaphragm, a significant toe region is seen in quasistatic as well as dynamic tests. However a large variation is seen in the toe region. The variation in toe strain can be expected on account of experimental variations in initial load/preconditioning and specimen dimensions like thickness and width and variations in the initial orientations of the fibres and in their initial slack. It was therefore decided to ignore the toe region, and examine the modulus only in the next region. Effective failure strain was then defined as the failure strain minus the toe strain. The effective failure strain is tabulated in Table 8 for all the tests. Table 9 shows the average failure strain (and its standard deviation) at different strain rates.

Table 8 – Effective failure strain in the different tests.

Serial no.	Test Id	Strain rate(/s)	Toe strain (%)	Final strain (%)	Effective failure strain
Quasi-static tensile tests					
1	HD1-01	1.00E-03	8.13	21.77	13.64
2	HD1-02	1.00E-03	9.86	21.04	11.18
3	HD1-03	1.00E-03	12.83	25.84	13.01
4	HD1-04	1.00E-03	8.71	24.64	15.93
5	HD5-03	1.00E-03	12.74	19.45	6.71
Dynamic tensile tests					
1	HD2-01	65	9.21	13.06	3.85
2	HD2-03	65	8.56	11.43.	2.87
3	HD2-05	67.86	7.75	12.10	4.33
4	HD2-04	125	9.24	20.37	11.13
5	HD2-06	130	21	28.83	7.83
6	HD2-07	130	8.04	16.76	8.72
7	HD5-04	130	14.72	28.11	13.39
8	HD5-06	136	14.71	20.70	5.98
9	HD2-09	180	20.14	30.04	10
10	HD3-01	190	10.75	19.69	8.94
11	HD3-02	192	25.36	34.2	8.84
12	HD6-01	190	7.48	20.41	12.93
13	HD6-02	192	6.9	18.75	11.85

Table 9 – Average effective failure strain and standard deviation at different strain rates.

Strain rate (/s)	Av. effective failure strain
Quasi-static tensile test	
1.00E−03	12.09 (±3.08)
Dynamic tensile test	
65	3.70 (±0.60)
130	9.65 (±2.60)
190	10.51 (±1.62)

Thus, Young's modulus as shown in Fig. 16(b) and effective failure strain as in Table 4 are recommended. This corresponds to a Young's Modulus of 12 MPa under quasi-static conditions, 64.6 MPa at a strain rate of 65/s, 50.10 MPa at a strain rate of 130/s and 38 MPa at a strain rate of 190/s; and an effective failure strain of 12.09%, 4%, 9.4% and 10.49% at these strain rates respectively.

4. Conclusion

This study presented a total of 18 uniaxial tensile tests conducted at four strain rates (up to 200/s) on fresh specimens of human diaphragm. Each specimen was tested until failure at one of the four strain rates (1e-3s^{-1}, 65 s^{-1}, 130 s^{-1} and 190 s^{-1}) using custom developed uniaxial quasistatic and dynamic tensile test set-ups. The data from the study showed that the response of human diaphragm in tension is nonlinear and strain rate dependent, with higher rate giving higher values of failure stress and failure strains. While the failure stress ranged from 1.17 MPa to 4.10 MPa and the

effective failure strains ranged from 3.79 to 12%, the elastic modulus changed from 12 MPa under quasi-static conditions to about 38 MPa at strain rates of 190/s. The loading curves exhibit multilinear behaviour (bilinear fit is being assumed). In summary, this study tries to provide biomechanical data that can be useful in the development of strain rate dependent material models and tissue level tolerance values to evaluate the injury risk in automotive collisions using human body finite element models.

Acknowledgement

The work was supported by a Grant from Mercedes Benz R&D India.

REFERENCES

Adegboye, V.O., Ladipo, J.K., Adebo, O.A., Brimmo, A.I., 2002. Diaphragmatic injuries. Afr. J. Med. Med. Sci. 31 (2), 149–153.

Ahmad, R., Suhail, M., Nafae, A., Khan, Q., Salam, P., Bashir, S., Nisar, Y., 2015. Isolated blunt traumatic diaphragmatic rupture in a case of situs inversus. Surg. Sci., 133–137.

Angelillo, M., Boriek, A.M., Rodarte, J.R., Wilson, T.A., 1997. Theory of diaphragm structure and shape. J. Appl. Physiol. 83 (5), 1486–1491.

Angelillo, M., Boriek, A.M., Rodarte, J.R., Wilson, T.A., 2000. Shape of the canine diaphragm. J. Appl. Physiol. 89 (1), 15–20.

Assari, S., Rachev, A., Darvish, K., 2014. High Rate Failure Properties of Aortic Tissue. pp. 1–11.

Augenstein, J., Perdeck, E., Bowen, J., Stratton, J., Singer, M., Horton, T., Steps, J., 1999. Injuries in near-side collisions. In: Annual Proceedings/Association for the Advancement of Automotive Medicine, 43, 139–158. Retrieved from ⟨http://www.ncbi.nlm.nih.gov/pmc/articles/PMC3400216/⟩.

Bartlett, C.S., 2003. Clinical update: gunshot wound ballistics. Clin. Orthop. Relat. Res. 408, 28–57.

Behr, M., Arnoux, P.J., Serre, T., Bidal, S., Kang, H.S., Thollon, L., Brunet, C., 2003. A human model for road safety: from geometrical acquisition to model validation with radioss. Comput. Methods Biomech. Biomed. Eng. 6 (4), 263–273, http://dx.doi.org/10.1080/1025584031000160608O.

Bir, C., Viano, D., King, A., 2004. Development of biomechanical response corridors of the thorax to blunt ballistic impacts. J. Biomech. 37 (1), 73–79.

Boriek, A.M., Hwang, W., Trinh, L., Rodarte, J.R., 2005. Shape and tension distribution of the active canine diaphragm. Am. J. Physiol. Regul. Integr. Comp. Physiol. 288 (4)http://dx.doi.org/10.1152/ajpregu.00499.2003.

Boriek, A.M., Kelly, N.G., Rodarte, J.R., Wilson, T.A., 2000. Biaxial constitutive relations for the passive canine diaphragm. J. Appl. Physiol. 89 (6), 2187–2190.

Bosanquet, D., Farboud, A., Luckraz, H., 2009. A review diaphragmatic injury. Respir. Med. CME 2 (1), 1–6, http://dx.doi.org/10.1016/j.rmedc.2009.01.002.

Boulanger, B.R., Milzman, D.P., Rosati, C., Rodriguez, A., 1993. A comparison of right and left blunt traumatic diaphragmatic rupture. J. Trauma 35 (2), 255–260.

Brown, B.J.B., C.B., A.W.T., A.P.J, W.G.P., A.W., K.A., 2014. Mechanical and histological characterization of trachea tissue subjected to blast-type pressures. Journal of Physics: Conference Series, 500(18), 182007. Retrieved from ⟨http://stacks.iop.org/1742-6596/500/i=18/a=182007⟩.

Brunon, A., Bruyere-Garnier, K., Coret, M., 2010. Mechanical characterization of liver capsule through uniaxial quasi-static tensile tests until failure. J. Biomech. 43 (11), 2221–2227, http://dx.doi.org/10.1016/j.jbiomech.2010.03.038.

Brunon, A., Bruyere-Garnier, K., Coret, M., 2011. Characterization of the nonlinear behaviour and the failure of human liver capsule through inflation tests. J. Mech. Behav. Biomed. Mater. 4 (8), 1572–1581, http://dx.doi.org/10.1016/j.jmbbm.2010.12.016.

Butler, D.L., Kay, M.D., Stouffer, D.C., 1986. Comparison of material properties in fascicle-bone units from human patellar tendon and knee ligaments. J. Biomech. 19 (6), 425–432, http://dx.doi.org/10.1016/0021-9290(86)90019-9.

Carew, T.E., Vaishnav, R.N., Patel, D.J., 1968. Compressibility of the arterial wall. Circ. Res. 23 (1), 61–68.

Carter, F.J., Frank, T.G., Davies, P.J., McLean, D., Cuschieri, A., 2001. Measurements and modelling of the compliance of human and porcine organs. Med. Image Anal. 5 (4), 231–236.

Cavanaugh, J., Walilko, T., 1996. Abdominal injury and response in side impact. In: Proceedings: Stapp Car. doi: 10.4271/962410.

Chawla, A., Mukherjee, S., Marathe, R., Karthikeyan, B., 2006. Determining Strain Rate Dependence of Human Body Soft Tissues Using a Split Hopkinson Pressure Bar. pp. 173–182.

Chawla, A., Mukherjee, S., Warhatka, H., Delhi, N., Malhotra, R., 2005. Dynamic Characterization of Bovine Medial Collateral Ligaments.

Choudhury, N., Bouchot, O., Rouleau, L., Tremblay, D., Cartier, R., Butany, J., Leask, R.L., 2009. Local mechanical and structural properties of healthy and diseased human ascending aorta tissue. Cardiovasc. Pathol. 18 (2), 83–91, http://dx.doi.org/10.1016/j.carpath.2008.01.001.

Christensen, M.B., Oberg, K., Wolchok, J.C., 2015. Tensile properties of the rectal and sigmoid colon: a comparative analysis of human and porcine tissue. SpringerPlus 4, 142, http://dx.doi.org/10.1186/s40064-015-0922-x.

Chung, J., Cavanaugh, J.M., King, A.I., Koh, S., 1999. SAE Technical Thoracic Injury Mechanisms and Biomechanical Responses in Lateral Velocity Pulse Impacts. SAE Tech. Pap., 724.

Cooper, G.J., Townend, D.J., Cater, S.R., Pearce, B.P., 1991. The role of stress waves in thoracic visceral injury from blast loading: modification of stress transmission by foams and high-density materials. J. Biomech. 24 (5), 273–285.

Covey, D.C., 2002. Blast and fragment injuries of the musculoskeletal system. J. Bone Jt. Surg. Am. Vol. 84-A (7), 1221–1234.

Decraemer, W.F., Maes, M.A., Vanhuyse, V.J., 1980. An elastic stress–strain relation for soft biological tissues based on a structural model. J. Biomech. 13 (6), 463–468, http://dx.doi.org/10.1016/0021-9290(80)90338-3.

Duprey, A., 2008. Mechanical properties of the aorta. The European Society for Vascular Surgery, 1–54. Retrieved from ⟨http://www.esvs.org/sites/default/files/image/Travelgrantreports/Duprey_Report.pdf⟩.

Edsberg, L.E., Mates, R.E., Baier, R.E., Lauren, M., 1999. Mechanical characteristics of human skin subjected to static versus cyclic normal pressures. J. Rehabil. Res. Dev. 36 (2), 133–141.

Egorov, V.I., Schastlivtsev, I.V., Prut, E.V., Baranov, A.O., Turusov, R.A., 2002. Mechanical properties of the human gastrointestinal tract. J. Biomech. 35.

Elhagediab A.M., Rouhana S.W., 1998. Patterns of abdominal injury in frontal automotive crashes. In: Proceedings of the 16th International ESV Conference Proceedings. pp. 327 – 337.

Favre, J.-P., Cheynel, N., Benoit, L., Favoulet, P., 2005. Traitement chirurgical des ruptures traumatiques du diaphragme. EMC – Chir. 2 (3), 242–251, http://dx.doi.org/10.1016/j.emcchi.2005.04.004.

Fung, Y.C., 1975. On mathematical models of stress-strain relationship for living soft tissues. Polym. Mech. 11 (5), 726–740, http://dx.doi.org/10.1007/BF00859649.

Holzapfel., G.A., 2000. Biomechanics of Soft Tissue, 7.

Gallagher, A., Annaidh, a.N., Bruyère, K., 2012. Dynamic tensile properties of human skin. In: Proceedings of IRCOBI Conference. pp. 494–502. ⟨http://doi.org/Irc-12-59⟩.

Ganpule, S., Alai, A., Plougonven, E., Chandra, N., 2013. Mechanics of blast loading on the head models in the study of traumatic brain injury using experimental and computational approaches. Biomech. Model. Mechanobiol. 12 (3), 511–531, http://dx.doi.org/10.1007/s10237-012-0421-8.

Gao, Z., Desai, J.P., 2010. Estimating zero strain states of very soft tissue under gravity loading using digital image correlation. Med. Image Anal. 14 (2), 126, http://dx.doi.org/10.1016/j.media.2009.11.002.

Grimal, Q., Gama, B.A., Naili, S., Watzky, A., Gillespie Jr., J.W., 2004. Finite element study of high-speed blunt impact on thorax: linear elastic considerations. Int. J. Impact Eng. 30 (6), 665–683, http://dx.doi.org/10.1016/j.ijimpeng.2003.08.002.

Gundiah, N., B Ratcliffe, M., Pruitt, L, A., 2007. Determination of strain energy function for arterial elastin: experiments using histology and mechanical tests. J. Biomech. 40 (3), 586–594, http://dx.doi.org/10.1016/j.jbiomech.2006.02.004.

Hanna, W.C., Ferri, L.E., Fata, P., Razek, T., Mulder, D.S., 2008. The current status of traumatic diaphragmatic injury: lessons learned from 105 patients over 13 years. Ann. Thorac. Surg. 85 (3), 1044–1048, http://dx.doi.org/10.1016/j.athoracsur.2007.10.084.

He, C.M., Roach, M.R., 1994. The composition and mechanical properties of abdominal aortic aneurysms. J. Vasc. Surg. 20 (1), 6–13.

Holzapfel G.A., 2004. Computational biomechanics of soft biological tissue. In: Encyclopedia of Computational Mechanics. John Wiley & Sons, Ltd doi: 10.1002/0470091355.ecm041.

Kara, E., Kaya, Y., Zeybek, R., Coskun, T., Yavuz, C., 2004. A case of a diaphragmatic rupture complicated with lacerations of stomach and spleen caused by a violent cough presenting with mediastinal shift. Ann. Acad. Med. Singap. 33 (5), 649–650.

Kemper A.R., Santago A.C., Stitzel J.D., Sparks J.L., Duma S.M., 2010. Biomechanical response of human liver in tensile loading. In: Proceedings of the Annals of Advances in Automotive Medicine/Annual Scientific Conference. Association for the Advancement of Automotive Medicine. Association for the Advancement of Automotive Medicine. Scientific Conference, 54, pp. 15–26.

Kemper, A.R., Santago, A.C., Stitzel, J.D., Sparks, J.L., Duma, S.M., 2012. Biomechanical response of human spleen in tensile loading. J. Biomech. 45 (2), 348–355, http://dx.doi.org/10.1016/j.jbiomech.2011.10.022.

Kenedi, R.M., 1971. Strength of biological materials. J. Anat. 108 (Pt 3), 582, http://dx.doi.org/10.1016/0021-9290(71)90027-3.

Kim, M.J., Druz, W.S., Danon, J., Machnach, W., Sharp, J.T., 1976. Mechanics of the canine diaphragm. J. Appl. Physiol. 41 (3), 369–382.

Lake, S.P., Miller, K.S., Elliott, D.M., Soslowsky, L.J., 2009. Effect of fiber distribution and realignment on the nonlinear and inhomogeneous mechanical properties of human supraspinatus tendon under longitudinal tensile loading. J. Orthop. Res. : Off. Publ. Orthop. Res. Soc. 27 (12), 1596, http://dx.doi.org/10.1002/jor.20938.

Laksari, K., Sadeghipour, K., Darvish, K., 2014. Mechanical response of brain tissue under blast loading. J. Mech. Behav. Biomed. Mater. 32, 132–144, http://dx.doi.org/10.1016/j.jmbbm.2013.12.021.

Manoogian, S.J., Bisplinghoff, J.A., McNally, C., Kemper, A.R., Santago, A.C., Duma, S.M., 2008. Dynamic tensile properties of human placenta. J. Biomech. 41 (16), 3436–3440, http://dx.doi.org/10.1016/j.jbiomech.2008.09.020.

Mansour, K.A., 1997. Trauma to the diaphragm. Chest Surg. Clin. North Am. 7 (2), 373–383.

Margulies, S.S., Lei, G.T., Farkas, G.A., Rodarte, J.R., 1994. Finite-element analysis of stress in the canine diaphragm. J. Appl. Physiol. 76 (5), 2070–2075.

Markogiannakis, H., Sanidas, E., Messaris, E., Koutentakis, D., Alpantaki, K., Kafetzakis, A., Tsiftsis, D., 2006. Motor vehicle trauma: analysis of injury profiles by road-user category. Emerg. Med. J: EMJ 23 (1), 27–31, http://dx.doi.org/10.1136/emj.2004.022392.

Mattucci, S.F.E., Moulton, J.A., Chandrashekar, N., Cronin, D.S., 2012. Strain rate dependent properties of younger human cervical spine ligaments. J. Mech. Behav. Biomed. Mater. 10, 216–226, http://dx.doi.org/10.1016/j.jmbbm.2012.02.004.

Mavrilas, D., Sinouris, E.A., Vynios, D.H., Papageorgakopoulou, N., 2005. Dynamic mechanical characteristics of intact and structurally modified bovine pericardial tissues. J. Biomech. 38 (4), 761–768, http://dx.doi.org/10.1016/j.jbiomech.2004.05.019.

McElhaney, J.H., 1966. Dynamic response of bone and muscle tissue. J. Appl. Physiol. 21 (4), 1231–1236.

McElwee, T.B., Myers, R.T., Pennell, T.C., 1984. Diaphragmatic rupture from blunt trauma. Am. Surg. 50 (3), 143–149.

Mihos, P., Potaris, K., Gakidis, J., Paraskevopoulos, J., Varvatsoulis, P., Gougoutas, B., Lapidakis, E., 2003. Traumatic rupture of the diaphragm: experience with 65 patients. Injury 34 (3), 169–172.

Miller, K., 2000. Biomechanics of soft tissues. Med. Sci. Monitor : Int. Med. J. Exp. Clin. Res. 6 (1), 158–167.

Miller, K., Chinzei, K., 1997. Constitutive modelling of brain tissue: experiment and theory. J. Biomech. 30 (11–12), 1115–1121.

Minns, R.J., Soden, P.D., Jackson, D.S., 1973. The role of the fibrous components and ground substance in the mechanical properties of biological tissues: a preliminary investigation. J. Biomech. 6 (2), 153–165, http://dx.doi.org/10.1016/0021-9290(73)90084-5.

Mohammadi, H., Bahramian, F., Wan, W., 2009. Advanced modeling strategy for the analysis of heart valve leaflet tissue mechanics using high-order finite element method. Med. Eng. Phys. 31 (9), 1110–1117, http://dx.doi.org/10.1016/j.medengphy.2009.07.012.

Mohan, D., Melvin, J.W., 1982. Failure properties of passive human aortic tissue. I–uniaxial tension tests. J. Biomech. 15 (11), 887–902.

Mohan, D., Melvin, J.W., 1983. Failure properties of passive human aortic tissue. II–Biaxial tension tests. J. Biomech. 16 (1), 31–44.

Murray, C.J.L., Lopez, A.D., 1996. The Global Burden of Disease: A Comprehensive Assessment of Mortality and Disability From Deceases, Injuries and Risk Factors in 1990 and Projected to 2010, 1. Harvard University Press1–35, http://dx.doi.org/10.1186/1471-2458-13-863.

Murray, J.A., Demetriades, D., Asensio, J.A., Cornwell 3rd, E.E., Velmahos, G.C., Belzberg, H., Berne, T.V., 1998. Occult injuries to the diaphragm: prospective evaluation of laparoscopy in penetrating injuries to the left lower chest. J. Am. Coll. Surg. 187 (6), 626–630.

Ottenio, M., Tran, D., Ní Annaidh, A., Gilchrist, M.D., Bruyère, K., 2015. Strain rate and anisotropy effects on the tensile failure characteristics of human skin. J. Mech. Behav. Biomed. Mater. 41, 241–250, http://dx.doi.org/10.1016/j.jmbbm.2014.10.006.

Ozpolat, B., Kaya, O., Yazkan, R., Osmanoglu, G., 2009. Diaphragmatic injuries: a surgical challenge. report of forty-one cases. Thorac. Cardiovasc. Surg. 57 (6), 358–362, http://dx.doi.org/10.1055/s-0029-1185579.

Patel, D.J., Janicki, J.S., Carew, T.E., 1969. Static anisotropic elastic properties of the aorta in living dogs. Circ. Res. 25 (6), 765–779.

Raghavan, M.L., Webster, M.W., Vorp, D.A., 1996. Ex vivo biomechanical behavior of abdominal aortic aneurysm: assessment using a new mathematical model. Ann. Biomed. Eng. 24 (5), 573–582.

Rashid, B., Destrade, M., Gilchrist, M.D., 2012. Mechanical characterization of brain tissue in compression at dynamic strain rates. J. Mech. Behav. Biomed. Mater. 10, 23–38, http://dx.doi.org/10.1016/j.jmbbm.2012.01.022.

Rashid, B., Destrade, M., Gilchrist, M.D., 2014. Mechanical characterization of brain tissue in tension at dynamic strain rates. J. Mech. Behav. Biomed. Mater. 33, 43–54, http://dx.doi.org/10.1016/j.jmbbm.2012.07.015.

Reber, P.U., Schmied, B., Seiler, C.A., Baer, H.U., Patel, A.G., Buchler, M.W., 1998. Missed diaphragmatic injuries and their long-term sequelae. J. Trauma 44 (1), 183–188.

Roberts, J.C., Merkle, A.C., Biermann, P.J., Ward, E.E., Carkhuff, B. G., Cain, R.P., O'Connor, J.V., 2007. Computational and experimental models of the human torso for non-penetrating ballistic impact. J. Biomech. 40 (1), 125–136, http://dx.doi.org/10.1016/j.jbiomech.2005.11.003.

Robin, S., 2001. Humos: human model for safety – a joint effort towards the development of refined human like car occupant models. In: Proceedings of the Stapp Car Crash Conference. 297. pp.1–9. Retrieved from ⟨http://www-nrd.nhtsa.dot.gov/pdf/nrd-01/esv/esv17/proceed/00129.pdffrom⟩.

Saraf, H., Ramesh, K.T., Lennon, A.M., Merkle, A.C., Roberts, J.C., 2007. Mechanical properties of soft human tissues under dynamic loading. J. Biomech. 40 (9), 1960–1967, http://dx.doi.org/10.1016/j.jbiomech.2006.09.021.

Scharff, J.R., Naunheim, K.S., 2007. Traumatic diaphragmatic injuries. Thorac. Surg. Clin. 17 (1), 81–85, http://dx.doi.org/10.1016/j.thorsurg.2007.03.006.

Sellier, K.G., Kneubuehl, B.P., 1994. Wound Ballistics and the Scientific Background. Elsevier. Retrieved from ⟨https://books.google.co.in/books?id=jZf1GaXQUvQC⟩.

Snedeker, J.G., Barbezat, M., Niederer, P., Schmidlin, F.R., Farshad, M., 2005. Strain energy density as a rupture criterion for the kidney: impact tests on porcine organs, finite element simulation, and a baseline comparison between human and porcine tissues. J. Biomech. 38 (5), 993–1001, http://dx.doi.org/10.1016/j.jbiomech.2004.05.030.

Snedeker, J.G., Niederer, P., Schmidlin, F.R., Farshad, M., Demetropoulos, C.K., Lee, J.B., Yang, K.H., 2005. Strain-rate dependent material properties of the porcine and human kidney capsule. J. Biomech. 38 (5), 1011–1021, http://dx.doi.org/10.1016/j.jbiomech.2004.05.036.

Sokolis, D.P., 2007. Passive mechanical properties and structure of the aorta: segmental analysis. Acta Physiol. 190 (4), 277–289, http://dx.doi.org/10.1111/j.1748-1716.2006.01661.x.

Song, B., Chen, W., Ge, Y., Weerasooriya, T., 2007. Dynamic and quasi-static compressive response of porcine muscle. J. Biomech. 40 (13), 2999–3005, http://dx.doi.org/10.1016/j.jbiomech.2007.02.001.

Strumpf, R.K., Humphrey, J.D., Yin, F.C., 1993. Biaxial mechanical properties of passive and tetanized canine diaphragm. Am. J. Physiol. 265 (2 Pt 2), H469–H475.

Takaza, M., Moerman, K.M., Gindre, J., Lyons, G., Simms, C.K., 2013. The anisotropic mechanical behaviour of passive skeletal muscle tissue subjected to large tensile strain. J. Mech. Behav. Biomed. Mater. 17, 209–220, http://dx.doi.org/10.1016/j.jmbbm.2012.09.001.

Taylor, P.A., Ludwigsen, J.S., Ford, C.C., 2014. Investigation of blast-induced traumatic brain injury. Brain Inj. 28 (7), 879–895, http://dx.doi.org/10.3109/02699052.2014.888478.

Thomas P., Frampton R., 1999. SAE Technical Injury Patterns in Side Collisions – A New Look with Reference to Current Test Methods and Injury Criteria. 724.

Thubrikar, M.J., Labrosse, M., Robicsek, F., Al-Soudi, J., Fowler, B., 2001. Mechanical properties of abdominal aortic aneurysm wall. J. Med. Eng. Technol. 25 (4), 133–142.

Umale, S., Deck, C., Bourdet, N., Dhumane, P., Soler, L., Marescaux, J., Willinger, R., 2013. Experimental mechanical characterization of abdominal organs: liver, kidney and spleen. J. Mech. Behav. Biomed. Mater. 17, 22–33, http://dx.doi.org/10.1016/j.jmbbm.2012.07.010.

Van Sligtenhorst, C., Cronin, D.S., Wayne Brodland, G., 2006. High strain rate compressive properties of bovine muscle tissue determined using a split Hopkinson bar apparatus. J. Biomech. 39 (10), 1852–1858, http://dx.doi.org/10.1016/j.jbiomech.2005.05.015.

Vorp, D.A., Schiro, B.J., Ehrlich, M.P., Juvonen, T.S., Ergin, M.A., Griffith, B.P., 2003. Effect of aneurysm on the tensile strength and biomechanical behavior of the ascending thoracic aorta. Ann. Thorac. Surg. 75 (4), 1210–1214.

Warhatkar H., Chawla A., Mukherjee S., 2009. Experimental study of variation between quasi-static and dynamic load deformation properties of bovine medial collateral ligaments rajesh malhotra. Seven. doi: 10.4271/2009-01-0392.

Yang, Z., Wang, Z., Tang, C., Ying, Y., 1996. Biological effects of weak blast waves and safety limits for internal organ injury in the human body. J. Trauma 40 (3 Suppl), S81–S84.

Yoganandan, N., Pintar, F.A., Gennarelli, T.A., Maltese, M.R., 2000. Patterns of abdominal injuries in frontal and side impacts. Annual Proceedings/Association for the Advancement of Automotive Medicine, 44, pp. 17–36. Retrieved from ⟨http://www.ncbi.nlm.nih.gov/pmc/articles/PMC3217390/⟩.

Zhang, W., Kassab, G.S., 2007. A bilinear stress–strain relationship for arteries. Biomaterials 28 (6), 1307–1315, http://dx.doi.org/10.1016/j.biomaterials.2006.10.022.